Spontaneous stacking faults in van der Waals heterostructures

G. Boussinot
Access e.V., Intzestrasse 5, 52072 Aachen, Germany
(Received 20 April 2016; revised manuscript received 22 July 2016; published 8 August 2016)

The rapid developments in the manipulation of two-dimensional monoatomic layers such as graphene or h-BN allow one to create heterostructures consisting of possibly many chemically different layers, stacked owing to van der Waals attraction. We propose a Frenkel-Kontorova model including a transverse degree of freedom in order to describe local deformations in these heterostructures. We study the case where two dissimilar monolayers are alternatively stacked, and find that stacking faults may emerge spontaneously for a large enough number of stacked layers as a result of the competition between adhesion and elastic energies. This symmetry-breaking transition should become of fundamental importance for the description of three-dimensional van der Waals heterostructures as soon as a precise control on the lattice orientation of the van der Waals layers is achieved.

DOI: 10.1103/PhysRevB.94.075410

I. INTRODUCTION

Since the discovery of the stability of the one-atom-thick carbon layer called graphene [1,2], an increasing number of other monolayers such as hexagonal boron nitride (h-BN), MoS_2, or WSe_2 have proven to be stable. Thanks to the van der Waals (vdW) attraction, responsible for example for the ability of a gecko to stick to a clean and flat ceiling [3], one may stack these chemically different monolayers and build a so-called "vdW heterostructure" (see [4] and references therein). Moreover, owing to the weakness of the vdW attraction, the layers may be stacked with almost any misorientation between their lattices, and progress concerning the control of this misorientation is ongoing [5,6]. Each vdW heterostructure, i.e., each stacking sequence, possesses unique physical properties and the physics of vdW heterostructures thus represents a new and extraordinarily large domain of research, which up to now has only scarcely been investigated. In the future, three-dimensional crystals consisting of a large number of stacked monolayers will be produced whose properties will be tuned by a precise scheme for the stacking sequence.

An especially important reason behind the investigations of vdW heterostructures concerns the possibility of tuning the fascinating electronic properties of graphene [2,7]. For example, an energy gap opens in its electronic spectrum when it interacts with h-BN [8–10]. This deviation from the spectrum of isolated graphene is due to small spatially varying deformations of the crystalline lattice. Although resulting in some elastic energy, these local deformations are favorable energetically because they allow a decrease in the interaction energy between layers; i.e., the adhesion energy between layers increases. This competition between elastic and adhesion energies arises in different contexts in surface science and the tool of choice to study it phenomenologically is the Frenkel-Kontorova (FK) model (see [11] and references therein).

Here we propose a FK model with a transverse degree of freedom to study vdW heterostructures. The local description of the deformation of the layers with respect to their stress-free state (when the layer is isolated) is provided by the usual in-plane displacement [12] supplemented by a transverse (or out-of-plane) displacement [13–16]. The particularity of the model is that, according for example to Ref. [17] concerning the interaction between graphene and h-BN, the relative in-plane displacement between layers influences the adhesion energy *and* the interlayer equilibrium distance. Although strain sharing between layers may allow their lattice to be in registry over the whole sample, we consider here the case where the lattices are incommensurate and build a so-called moiré periodic pattern [5,18] with an incommensurability defect, i.e., a dislocation (also called a soliton or a kink in the frame of the classical FK model [11]), in each unit cell. Moreover, due to incommensurability, the whole landscape of the adhesion potential between layers is explored and the optimum distance between them varies within a moiré unit cell. This effect is the key ingredient for the corrugation of the layers in the transverse direction [19].

Our investigation focuses on a structure where two dissimilar monolayers A and B are alternatively stacked building a sequence A-B-A-B-A.... For a small enough number N of stacked layers, the incommensurability defects are aligned vertically and sit on top of each other as a result of adhesion energy minimization. This vertical alignment is associated with an elastic energy in the layers (bending and stretching) that increases with N. Above a critical N, the vertical alignment is destabilized and, as we will see in this article, the incommensurability defects then align obliquely yielding stacking faults in the vdW heterostructure. The article is organized as follows. We first present the FK model and its assumptions. Second, we present the numerical results that evidence the symmetry-breaking transition yielding stacking faults in the vdW heterostructure. We then discuss these results and finally conclude.

II. FRENKEL-KONTOROVA MODEL

FK models were used to study or invoked to explain commensurate-incommensurate transitions in bilayer graphene [12] and in the graphene/h-BN system [5]. Here, we consider a vdW heterostructure consisting of N stacked monolayers numerated by the integer n. We introduce the space-dependent in-plane displacement $u_n(x)$ in layer n and the space-dependent position of the nth layer $v_n(x)$ in the direction perpendicular to the layers. As mentioned in the Introduction, the energy of the heterostructure consists of an adhesion energy between layers and an elastic energy due to their deformation. For the adhesion part, we use an additive

ansatz such that the total potential interaction energy in the heterostructure $E_{\rm adh}$ is calculated as a sum over all pairs of layers, i.e.,

$$E_{\rm adh} = \sum_{n=1}^{N} \sum_{m>n} E_{m,n}^{\rm adh}, \tag{1}$$

where $E_{m,n}^{\rm adh}$ is the pair-interaction adhesion potential between layer m and layer n. Moreover, we assume that the deformation of the monolayers is small, i.e., $u_n'(x) \ll 1$ and $v_n'(x) \ll 1$. This means that the displacements are changing appreciably on a scale that is much larger than the atomic distance, and it allows us to consider that the pair-interaction potential is a simple integral over the space of a local potential energy [19]:

$$E_{m,n}^{\rm adh} = \int_x f_{m,n}(x)dx, \tag{2}$$

where $f_{m,n}(x)$ is the local adhesion potential between layer n and layer m that *a priori* depends on their relative in-plane displacement $u_n(x) - u_m(x)$ and on their distance $|v_n(x) - v_m(x)|$. As mentioned in the Introduction, the adhesion potential between a graphene layer and a h-BN layer was calculated using DFT calculations [17]. These calculations are performed within a random phase approximation to treat the long-range electronic correlations that are responsible for the vdW attraction. As a function of the distance between the layers, several stacking configurations (relative in-plane displacement between the layers) were investigated and the adhesion curves present features that should be incorporated qualitatively in our model. In particular, the adhesion energy and the equilibrium distance between layers depend on the stacking configuration. However, the dependence on the stacking configuration of the pair-interaction potential is a result of short-range electrostatic interactions and therefore concerns only adjacent layers. Here, we model this adhesion behavior using a Lennard-Jones-type potential and for the in-plane displacement dependence, like in the usual FK models, we use a sinusoidal potential:

$$f_{m,n}(x) = \frac{r^\alpha\{1 - a\delta_{m,n\pm1}\cos 2\pi[u_n(x) - u_m(x)]\}}{|v_n(x) - v_m(x)|^\alpha} - \frac{r^\beta}{|v_n(x) - v_m(x)|^\beta}, \tag{3}$$

where $\alpha > \beta > 0$. The distinction between adjacent and nonadjacent layers is provided by the Kronecker symbol $\delta_{m,n\pm1}$ that equals 1 if $m = n + 1$ or $m = n - 1$ and equals 0 otherwise. The characteristic distance of this interaction is r and a represents the amplitude of the sinusoidal potential. Here, the lengths are scaled by an arbitrary atomic distance that defines a reference lattice used later on to calculate the elastic energy in the layers. We assume for simplicity that the pair-interaction potential is independent of the chemical nature of the layers, and thus consider n- and m-independent r,α,β, and a. In Fig. 1, we present $f_{m,n}$ as a function of $v/r = |v_m - v_n|/r$ for $u = u_m - u_n = 0$ and $u = 0.5$ (compare with Fig. 2 in [17]). The parameters of the Lennard-Jones potential are here $\alpha = 9, \beta = 3$, and $a = 0.5$.

Let us now turn to the description of the elastic energy stored in the layers due to their deformation. We consider two types of

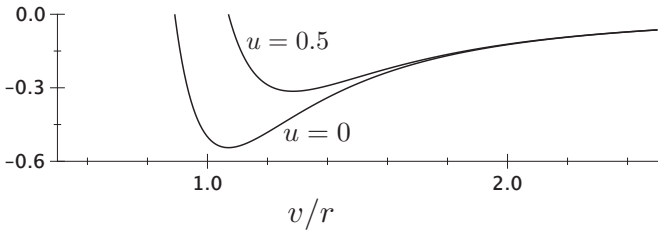

FIG. 1. Pair-interaction potential in Eq. (3) (with $\alpha = 9, \beta = 3$, and $a = 0.5$) between two layers separated by a distance $v = |v_n - v_m|$, and presenting a difference of in-plane displacement $u = u_n - u_m = 0$ and $u = 0.5$.

deformation: stretching and bending. As mentioned just above, we calculate the elastic energy using a reference lattice of arbitrary lattice parameter with which we scale all lengths. The (normalized) equilibrium lattice parameter b_n in layer n defines an equilibrium deformation $\epsilon_n = b_n - 1$. We assume that the moiré unit cell may present a deformation $\bar{\epsilon}$, i.e., a contraction $\bar{\epsilon} < 0$ or a dilatation $\bar{\epsilon} > 0$. The field $u_n(x)$ then represents the in-plane displacement in layer n relative to the deformed lattice having a lattice parameter $1 + \bar{\epsilon}$. The bond length may thus be written $l_n(x) = [\{1 + \bar{\epsilon} + u_n'(x)\}^2 + \{v_n'(x)\}^2]^{1/2} \approx 1 + \bar{\epsilon} + u_n'(x) + [v_n'(x)]^2/2$ and the stretching energy density in layer n at position x is proportional to $[l_n(x) - b_n]^2$. On the other hand, the bending energy is proportional to the square of the curvature of the layer, i.e., $[v_n''(x)]^2$. We thus finally write the elastic energy density at position x in layer n as

$$e_n^{\rm el}(x) = \frac{W^2}{2}[\{l_n(x) - b_n\}^2 + B\{v_n''(x)\}^2] \approx \frac{W^2}{2}\left[\left\{\bar{\epsilon} + u_n'(x) - \epsilon_n + \frac{[v_n'(x)]^2}{2}\right\}^2 + B\{v_n''(x)\}^2\right].$$

The parameter W represents the ratio between the elastic energy scale (the elastic constant) and the adhesion energy scale [taken as unity according to Eq. (3)]. The parameter B stands for a bending coefficient. Here, for simplicity again, we do not take into account the difference of elastic constant and bending coefficient between layers in the heterostructure. The total elastic energy in the system therefore reads

$$E_{\rm el} = \sum_{n=1}^{N} \int_x e_n^{\rm el}(x)dx. \tag{4}$$

Finally the total energy of our system is the sum of the adhesion energy and the elastic energy:

$$E = E_{\rm adh} + E_{\rm el}. \tag{5}$$

For a vdW heterostructure where the chemical bonding within the layers is much stronger than the one in the transverse direction (vdW bonding), the coefficient W is a large number. Let us note that $W \gg 1$ is actually a prerequisite to the conditions of small deformations $u_n'(x) \ll 1$ and $v_n'(x) \ll 1$, that allow us to write the adhesion energy in the vdW heterostructure in the simple form of Eqs. (1) and (2). Moreover, as mentioned in the Introduction, we assume incommensurable layers and the equilibrium structure presents a periodic moiré pattern. The periodicity of the moiré pattern, here the length of the moiré

cell, should be much larger than the atomic distance in order for the spatial derivatives of the displacements to be much smaller than unity. In the case that we study in the following with a single lattice misfit parameter ϵ, the length of the moiré cell is $1/\epsilon$. Thus $\epsilon \ll 1$ is also a prerequisite to the small deformation conditions.

Let us finally note that, in virtue of the small deformation conditions, the electronic degrees of freedom are effectively incorporated in the adhesion potential energy and in the elastic energy separately. More precisely, we neglect the influence of strain on the interaction energy between layers, and we consider that the elastic energy may be calculated in the same way as for an isolated layer.

III. NUMERICAL RESULTS

Let us now present numerical results for the equilibrium, i.e., $\delta E/\delta u_n(x) = \delta E/\delta v_n(x) = 0$, in a heterostructure where $\epsilon_n = -\epsilon = -0.01$ for even $n = 2p$ and $\epsilon_n = 0$ for odd $n = 2p+1$ (p is an integer). We assume that an external force is imposed such that $\bar{\epsilon} = 0$. We consider a periodic moiré pattern of period $1/\epsilon = 100$, and boundary conditions for the in-plane displacement of the form $u_n(1/\epsilon) = u_n(0)$ for odd n and $u_n(1/\epsilon) = u_n(0) - 1$ for even n are applied. For the transverse displacement, we use $v_n(1/\epsilon) = v_n(0)$ and $v_n(1+1/\epsilon) = v_n(1)$ (the latter condition being required for the bending term in the elastic energy that presents a higher order derivative compared to stretching) for all n. We choose $W = 50, B = 1$ and use a pair-interaction potential where $\alpha = 9, \beta = 3$ [20,21], and $a = 0.5$. Our potential is thus precisely the one corresponding to Fig. 1, and we use a characteristic length $r = 1$. Note that our choice for a enhances the differences of adhesion energy and equilibrium interlayer distance within a moiré cell compared to a realistic system like graphene/h-BN [17].

First, we present in Fig. 2 the equilibrium displacements in the case $N = 5$. We see that the equilibrium state is highly symmetric. In the left panel, we present the in-plane displacements $u_n(x)$ and evidence the incommensurability defect in each layer that takes the form of relatively well defined partial dislocations in the inner layers $n = 2,3,4$ (in the outer layers $n = 1$ and $n = 5$ the profile is more smooth). They have a Burgers vector $+1/2$ for odd n and $-1/2$ for even n. The partial dislocations are all centered at $x = 1/(2\epsilon) = 50$ and are thus aligned vertically. They separate a region where $u_n(x) = -\epsilon x/2$ from a region where $u_n(x) = -\epsilon x/2 - (-1)^n/2$. In each of these two regions, strain is shared equally by the two kinds of monolayers (because the difference of elastic constant W between layers is neglected) and the two lattices are locally commensurate. This is illustrated by the dashed lines. In the right panel in Fig. 2, we present the position of the layers in the transverse direction $v_n(x)$. We see that the distance between layers varies with the horizontal coordinate x and is larger at $x = 50$. This is the consequence of the variation of equilibrium interlayer distance with the relative in-plane displacement between layers (see Fig. 1), that is an integer at $x = 0$ and $x = 100$ and a half-integer at $x = 50$ (see left panel in Fig. 2). This leads to a uneven distribution of elastic energy in the vdW heterostructure. Indeed, since the corrugation of the layers leads to some stretching and some bending energies, we see for example that the elastic energy in layers $n = 1$ and $n = 5$ is larger than in layer $n = 3$.

When increasing N, we found that the highly symmetric state, presented above for $N = 5$, is destabilized. While the high-symmetry state is still stable at $N = 9$, it is unstable at $N = 11$. Then, a state with a lower degree of symmetry is the equilibrium state and we present it in Fig. 3. In the left panel, we present the in-plane displacement in each layer (denoted by their corresponding n in the figure). While again the in-plane displacement exhibits a smoother behavior in the outer layers $n = 1$ and $n = 11$ (represented in red), the partial dislocations in the inner layers are no longer centered at $x = 50$ as for the high-symmetry state, and they are aligned

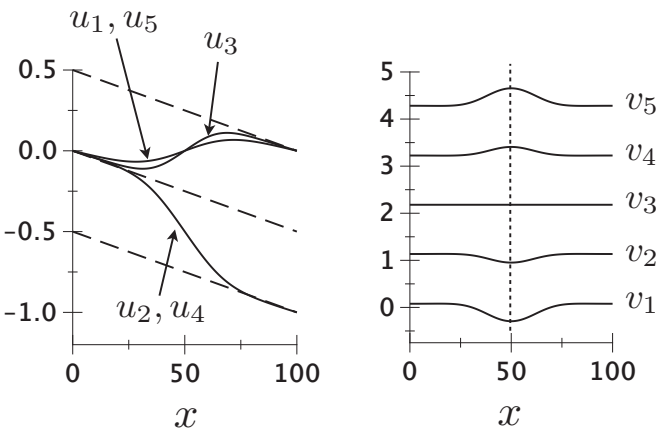

FIG. 2. Equilibrium displacements for $N = 5$. Left: in-plane displacements exhibiting incommensurability defects, i.e., partial dislocations, that are centered at $x = 50$. Right: position of the layers in the transverse direction. The vertical alignment of the partial dislocations is illustrated by the dashed line.

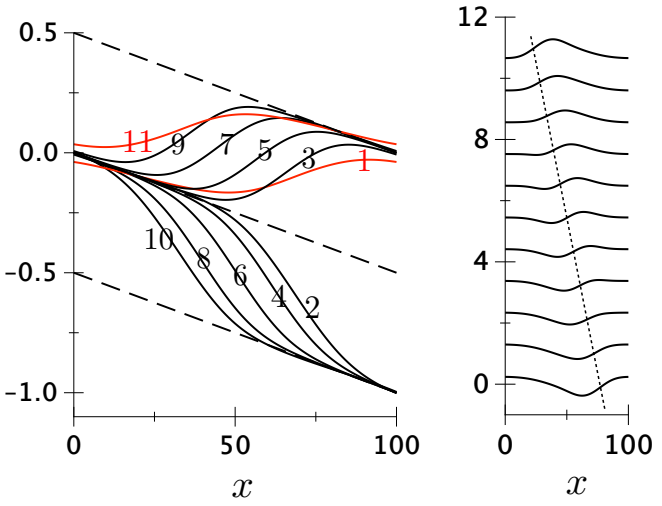

FIG. 3. Equilibrium displacements for $N = 11$. Left: in-plane displacements with their corresponding n (the outer layers $n = 1$ and $n = 11$ are in red). Right: position of the layers in the transverse direction (same order in the numbering of the layers as in Fig. 2). The oblique alignment of the partial dislocations yielding a stacking fault in the vdW heterostructure is illustrated by the dashed line.

obliquely. In the right panel in Fig. 3, we present the transverse position of the layers $v_n(x)$ (the same order in the numbering is used as in Fig. 2). We see that this new low-symmetry state allows for a more even distribution of strain in the vdW heterostructure as compared to the high-symmetry state; i.e., all layers are corrugated in the low-symmetry state. As before, the in-plane displacements are $u_n(x) = -\epsilon x/2$ on the left side of the line of dislocations and $u_n(x) = -\epsilon x/2 - (-1)^n/2$ on the right side. Since the line of dislocations is now oblique, it can be assimilated to a stacking fault. This is for example illustrated by the fact that $u_3(x = 50) \simeq u_9(x = 50) - 1/2$. This stacking fault emerges spontaneously as a result of the accumulation of strain in the vdW heterostructure, and the strain release is associated with an increase in the interaction energy between layers. It is important to mention that the symmetry-breaking transition that leads to the emergence of stacking faults does not take place if the transverse degree of freedom is frozen, i.e., if v_n does not depend on x. In Fig. 4, we present schematically the stacking fault within a moiré cell ($0 \leqslant x \leqslant 1/\epsilon$) for a heterostructure comprising two dissimilar layers (in color black and red) and $N = 20$ layers. The horizontal lines represent the strong intralayer bonding. Within the moiré cell, the vdW heterocrystal is built out of two regions, separated by the stacking fault, where the vdW layers share strain and are locally commensurate. The lattices in these two regions present a relative in-plane displacement $1/2$ between them (illustrated by the vertical blue line). An important remark concerns the general case where the two kinds of monolayers have different elastic constant, i.e., $W_n = w_0 + (-1)^n w_1$. In this case, the strain-sharing process yields a strain $\alpha = [1 + 2w_0 w_1/(w_0^2 + w_1^2)]\epsilon/2$ in locally commensurate regions. Then the partial dislocations have a Burgers vector equal to $\delta = \alpha/\epsilon - 1$ (i.e., $-1/2$ in the case $w_1 = 0$ in Fig. 4) for $n = 2p$ and equal to $1 + \delta$ (i.e., $+1/2$ for $w_1 = 0$) for $n = 2p + 1$. Thus if the in-plane displacement obeys $u_n = -\alpha x$ on the left side of the stacking fault, it obeys $u_{2p} = -\alpha x + \delta$ and $u_{2p+1} = -\alpha x + 1 + \delta$ on the right side. We are then left with a stacking fault that separates locally commensurate regions presenting between them an in-plane shift distance $|\delta| \in [0,1]$ that depends on w_1/w_0.

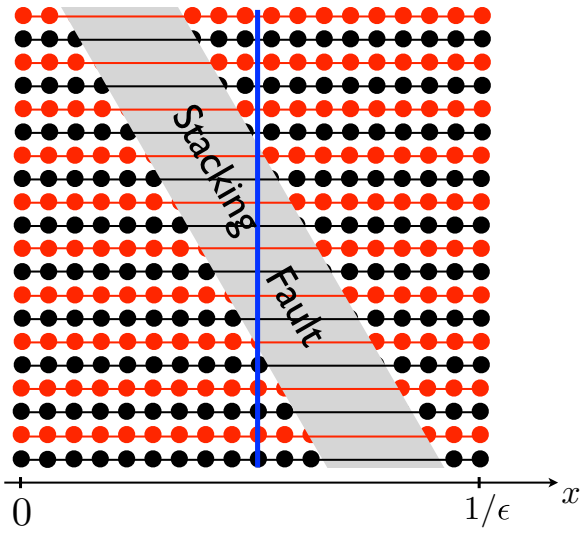

FIG. 4. Schematics of a stacking fault within a moiré cell in a vdW heterostructure comprising two dissimilar layers (in black and red). The horizontal lines represent the strong intralayer bonding. Within the moiré cell, the vdW heterocrystal is built out of two regions, separated by the stacking fault, where the layers share strain and are commensurate. The lattices in these two regions present a relative in-plane displacement 1/2 illustrated by the vertical blue line.

IV. DISCUSSION

The low-symmetry state with a stacking fault is actually degenerate. If the position of the partial dislocation in layer n at equilibrium is x_n, then the equilibrium state with $1/\epsilon - x_n$ is equivalent. In an extended system at nonzero temperature, these two different equilibrium low-symmetry states should thus coexist yielding domain boundaries whose properties should be investigated in the future.

We have made a simulation with $N = 32$ and found that the angle made by the oblique line of partial dislocations is the same as for $N = 11$. We thus conclude that this angle is a property of the system that should depend on ϵ, W, B and the pair-interaction potential rather than on N. The investigation of such a dependence is beyond the scope of this article but will represent a crucial piece of work for a deep understanding of the spontaneous emergence of stacking faults in vdW heterostructures. Since the angle does not depend on the number of stacked layer N, we may infer that large-scale vdW heterostructures with $N \gg 1$ should consist of a succession of oblique stacking faults depicted in Fig. 5 in the same way as in Fig. 3 with dashed lines. The locally commensurate regions separated by stacking faults may then be represented when $N \gg 1$ by the integer m (see Fig. 5) and the in-plane displacement obeys $u_{2p} = -\alpha x + m\delta$ and $u_{2p+1} = -\alpha x + m(1 + \delta)$ in the general case of different elastic constants presented in the previous section.

Let us now discuss the relevance of the present study to three-dimensional experimental situations. Let us first note that the emergence of stacking faults as a symmetry-breaking process due to strain energy release should occur also in the case of a heterostructure deposited on a substrate. The influence of the latter should concern only the layers in the vicinity of the substrate, in a rather similar way as the vacuum leading to a smoother in-plane displacement for $n = 1$ and $n = 11$ in Fig. 3. Second, as mentioned in the Introduction, the lattice orientation of the layers is a degree of freedom

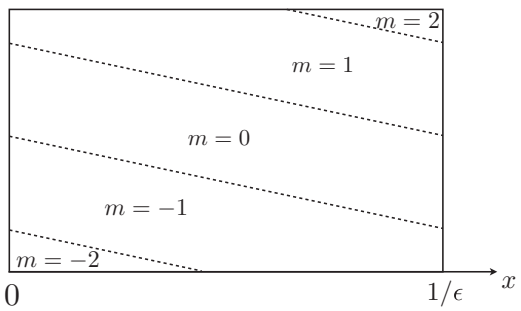

FIG. 5. Schematics of the stacking fault sequence (oblique dashed lines) in large-scale vdW heterostructure for $N \gg 1$.

in vdW heterostructures. For example, when one stacks a graphene layer on top of another graphene layer but with a different orientation (twisted graphene), a moiré pattern arises and the misorientation angle between layers plays the role of the lattice misfit used in this article. Since here we have used a single lattice misfit ϵ, our setup thus mimics a heterostructure with, for example, the following: for odd n, graphene layers orientated with a certain reference angle θ; for even n, graphene layers oriented with an angle δ such that $|\delta - \theta| \ll 1$. In this respect, the sequence of stacking faults described in this article shall be evidenced as a macroscopic state in the future when a precise control of the layers' lattice orientation is achieved. However, for the moment, since the layers may present local fluctuations in their orientation [22] at elevated temperatures, we can thus conceive that stacking faults may develop locally in these cases. Another possible experimental situation concerns graphene/h-BN. In this case, even if all layers are oriented in the same way, the system may exhibit a moiré pattern due to a lattice misfit (of order 2%). In Ref. [17], the optimum common lattice parameter due to strain sharing and the corresponding elastic energy for macroscopic commensuration were actually calculated. The authors found that the commensurate state is close in energy to the incommensurate state with a moiré pattern. One may thus expect that, at finite temperature, commensurate and incommensurate regions would coexist in graphene/h-BN heterostructures, and that the spontaneous emergence of stacking faults described in this article may occur when the heterostructure comprises a large number of stacked layers. This should greatly influence the physical properties of the heterostructure. However, for both graphene/h-BN and twisted graphene, we do not know yet which topology should be expected for these cases of hexagonal lattices.

V. SUMMARY

We have presented a Frenkel-Kontorova model with a transverse degree of freedom for van der Waals heterostructures. This model allows us to study local deformations within the two-dimensional van der Waals layers, these deformations being known to greatly influence their physical properties such as the optoelectronic ones. We study a heterostructure where two dissimilar monolayers are alternatively stacked and we find, for a large enough number of stacked layers, a spontaneous emergence of stacking faults. This symmetry-breaking transition is a result of the competition between adhesion and elastic energies and should greatly influence the physical properties of three dimensional van der Waals heterostructures for which a control on the layers' lattice orientation is achieved.

ACKNOWLEDGMENT

The author thanks E. A. Brener for always valuable discussions.

[1] K. S. Novoselov, D. Jiang, F. Schedin, T. J. Booth, V. V. Khotkevich, S. V. Morozov, and A. K. Geim, Proc. Natl. Acad. Sci. USA **102**, 10451 (2005).
[2] A. H. Castro-Neto, F. Guinea, N. M. R. Peres, K. S. Novoselov, and A. K. Geim, Rev. Mod. Phys. **81**, 109 (2009).
[3] K. Autumn, Y. A. Liang, S. T. Hsieh, W. Zesch, W. P. Chan, T. W. Kenny, R. Fearing, and R. J. Full, Nature (London) **405**, 681 (2000).
[4] A. K. Geim and I. V. Grigorieva, Nature (London) **499**, 419 (2013).
[5] C. R. Woods, L. Britnell, A. Eckmann, R. S. Ma, J. C. Lu, H. M. Guo, X. Lin, G. L. Yu, Y. Cao, R. V. Gorbachev, A. V. Kretinin, J. Park, L. A. Ponomarenko, M. I. Katsnelson, Yu. N. Gornostyrev, K. Watanabe, T. Taniguchi, C. Casiraghi, H.-G. Gao, A. K. Geim, and K. S. Novoselov, Nat. Phys. **10**, 451 (2014).
[6] S. Tang, H. Wang, Y. Zhang, A. Li, H. Xie, X. Liu, L. Liu, T. Li, F. Huang, X. Xie, and M. Jiang, Sci. Rep. **3**, 2666 (2013).
[7] K. S. Novoselov, A. K. Geim, S. V. Morozov, D. Jiang, M. I. Katsnelson, I. V. Grigorieva, S. V. Dubonos, and A. A. Firsov, Nature (London) **438**, 197 (2005).
[8] G. Giovannetti, P. A. Khomyakov, G. Brocks, P. J. Kelly, and J. van den Brink, Phys. Rev. B **76**, 073103 (2007).
[9] P. San-Jose, A. Gutiérrez-Rubio, M. Sturla, and F. Guinea, Phys. Rev. B **90**, 075428 (2014); **90**, 115152 (2014).
[10] M. Neek-Amal and F. M. Peeters, Appl. Phys. Lett. **104**, 173106 (2014).
[11] O. M. Braun and Y. S. Kivshar, *The Frenkel-Kontorova Model: Concepts, Methods, and Applications* (Springer-Verlag, Berlin, 2004).
[12] A. M. Popov, I. V. Lebedeva, A. A. Knizhnik, Y. E. Lozovik, and B. V. Potapkin, Phys. Rev. B **84**, 045404 (2011).
[13] O. M. Braun and Y. S. Kivshar, Phys. Rev. B **44**, 7694 (1991).
[14] O. M. Braun, O. A. Chubykalo, Y. S. Kivshar, and L. Vázquez, Phys. Rev. B **48**, 3734 (1993).
[15] O. M. Braun and M. Peyrard, Phys. Rev. B **51**, 17158 (1995).
[16] O. M. Braun, T. Dauxois, and M. Peyrard, Phys. Rev. B **54**, 313 (1996).
[17] B. Sachs, T. O. Wehling, M. I. Katsnelson, and A. I. Lichtenstein, Phys. Rev. B **84**, 195414 (2011).
[18] A. Summerfield, A. Davies, T. S. Cheng, V. V. Korolkov, Y. Cho, C. J. Mellor, C. T. Foxon, A. N. Khlobystov, K. Watanabe, T. Taniguchi, L. Eaves, S. V. Novikov, and P. H. Beton, Sci. Rep. **6**, 22440 (2016).
[19] H. Kumar, D. Er, L. Dong, J. Li, and V. Shenoy, Sci. Rep. **5**, 10872 (2015).
[20] J. F. Dobson, A. White, and A. Rubio, Phys. Rev. Lett. **96**, 073201 (2006).
[21] Z. H. Aitken and R. Huang, J. Appl. Phys. **107**, 123531 (2010).
[22] J. S. Alden, A. W. Tsen, P. Y. Huang, R. Hovden, L. Brown, J. Park, D. A. Muller, and P. L. McEuen, Proc. Natl. Acad. Sci. USA **110**, 11256 (2013).